AIAA 2001–2571

Distributed Relaxation for Conservative Discretizations

Boris Diskin
ICASE/NASA Langley Research Center, Hampton, VA 23681

James L. Thomas
NASA Langley Research Center, Hampton, VA 23681

15th AIAA Computational Fluid Dynamics Conference
June 11–14, 2001/Anaheim, CA

Distributed Relaxation for Conservative Discretizations

Boris Diskin *
ICASE/NASA Langley Research Center, Hampton, VA 23681

James L. Thomas†
NASA Langley Research Center, Hampton, VA 23681

A multigrid method is defined as having textbook multigrid efficiency (TME) if the solutions to the governing system of equations are attained in a computational work that is a small (less than 10) multiple of the operation count in one target-grid residual evaluation. The way to achieve this efficiency is the distributed relaxation approach. TME solvers employing distributed relaxation have already been demonstrated for *nonconservative* formulations of high-Reynolds-number viscous incompressible and subsonic compressible flow regimes. The purpose of this paper is to provide foundations for applications of distributed relaxation to conservative discretizations. A direct correspondence between the primitive variable interpolations for calculating fluxes in conservative finite-volume discretizations and stencils of the discretized derivatives in the nonconservative formulation has been established. Based on this correspondence, one can arrive at a conservative discretization which is very efficiently solved with a nonconservative relaxation scheme and this is demonstrated for conservative discretization of the quasi one-dimensional Euler equations. Formulations for both staggered and collocated grid arrangements are considered and extensions of the general procedure to multiple dimensions are discussed.

Introduction

Full multigrid (FMG) algorithms[1,2,9,18,22,23] are the fastest solvers for elliptic problems. These algorithms can solve a general discretized elliptic problem to the discretization accuracy in a computational work that is a small (less than 10) multiple of the operation count in one target-grid residual evaluation. Such efficiency is known as textbook multigrid efficiency (TME).[3] The difficulties associated with extending TME for solution of the Reynolds-averaged Navier-Stokes (RANS) equations relate to the fact that the RANS equations are a system of coupled nonlinear equations that is not, even for subsonic Mach numbers, fully elliptic, but contain hyperbolic partitions. TME for the RANS simulations can be achieved if the different factors contributing to the system could be separated and treated optimally, e.g., by multigrid for elliptic factors and by downstream marching for hyperbolic factors. The way to separate the factors is the distributed relaxation approach proposed earlier.[1,2] Usually, distributed relaxation can be applied throughout the entire domain having the full effect away from discontinuities (shocks, slip lines) in the regular (smoothly varying) flow field. Some local relaxation sweeps should be applied in these special regions after (and perhaps before) the distributed relaxation pass to reduce residuals to the average level characterizing the regular flow field. The general framework for achieving TME in large-scale computational fluid dynamics (CFD) applications has been discussed.[6,21]

The approach to the solution of the RANS equations proposed in this paper is based on an FMG algorithm with multigrid cycles employing distributed relaxation. It is envisioned that the FMG-1 algorithm (an algorithm with one multigrid cycle per level) will provide solutions with algebraic error below the level of the discretization error. Another useful characteristic of the solution process is a possibility to rapidly converge residuals to machine zero. The latter property is not necessary for achieving TME, but it is highly favored in practical applications.

The distributed relaxation approach relies on a principal linearization of the governing system of nonlinear equations. The principal linearization of a *scalar* equation contains the terms that make a major contribution to the residual per a unit change. The principal terms thus generally depend on the scale, or mesh size, of interest. For example, the discretized highest derivative terms are principal on grids with small enough mesh size. For a discretized *system* of differ-

*Staff Scientist, ICASE, (email: bdiskin@icase.edu). This research was supported by the National Aeronautics and Space Administration under NASA Contract No. NAS1-97046 while the author was in residence at the Institute for Computer Applications in Science and Engineering (ICASE), NASA Langley Research Center, Hampton, Virginia 23681-2199.

†Computational Modeling and Simulation Branch, Mail Stop 128, NASA Langley Research Center, Hampton, Virginia 23681 (email: j.l.thomas@larc.nasa.gov).

ential equations, the principal terms are those that contribute to the principal terms of the *determinant* of the matrix operator.

Development of a solution method for the governing RANS system can be significantly simplified if the target discretization possesses two properties: (1) The discretization of the corresponding principally linearized system is factorizable,[2,3,16,17] i.e., the determinant of the principal part of the discrete matrix operator can be represented as a product of discrete scalar factors, each of them approximating a corresponding factor of the differential matrix operator determinant. (2) The obtained scalar factor discretizations should reflect the physical anisotropies and be efficiently solvable. These two properties are not necessarily required for convergence of the algebraic errors in the FMG-1 algorithm, but they are very important for ensuring a fast residual convergence and providing accurate solutions.

Appropriate choices of factorizable discretizations for *nonconservative* formulations and textbook efficient multigrid solvers employing distributed relaxation have already been demonstrated for high-Reynolds-number viscous incompressible[7,20] and subsonic compressible[19] flow regimes. An example of the distributed relaxation involved in calculation of the Euler flow with shock has been demonstrated;[21] the finite-volume collocated-grid discretization scheme used in[21] was a standard flux-differencing splitting scheme of Roe.[15] Applied to a one-dimensional problem, the scheme is factorizable and provides reasonable approximations for the determinant factors. However, in multiple dimensions, the scheme is not factorizable, and other (factorizable) schemes should be considered. The purpose of this paper is to provide foundations for applying distributed relaxation to conservative discretizations of the Euler equations corresponding to factorizable discrete schemes.

The present material is organized in the following order: First, the Euler equations for inviscid compressible flow problems are defined. Secondly, the idea of distributed relaxation is briefly explained from both a differential and a discrete viewpoint. The attributes of a desired nonconservative Euler-system discretization scheme are discussed and a model problem, the one-dimensional Euler equations, is used to illustrate the derivation of conservative discretizations corresponding to a given nonconservative schemes. Numerical tests are reported for a collocated grid scheme for subsonic quasi-one-dimensional flow. Finally, concluding remarks are given.

Euler Equations

The time-dependent three-dimensional Euler system of compressible flow equations can be written as

$$\partial_t \mathbf{Q} + \mathbf{R} = 0, \tag{1}$$

where the conserved variables are $\mathbf{Q} \equiv (\rho u, \rho v, \rho w, \rho, \rho E)^T$, representing the momentum vector, density, and total energy per unit volume, and

$$\mathbf{R}(\mathbf{Q}) \equiv \partial_x \mathbf{F}(\mathbf{Q}) + \partial_y \mathbf{G}(\mathbf{Q}) + \partial_z \mathbf{H}(\mathbf{Q}), \tag{2}$$

$$\mathbf{F}(\mathbf{Q}) = \begin{pmatrix} \rho u^2 + p \\ \rho uv \\ \rho uw \\ \rho u \\ \rho uE + up \end{pmatrix}, \quad \mathbf{G}(\mathbf{Q}) = \begin{pmatrix} \rho uv \\ \rho v^2 + p \\ \rho vw \\ \rho v \\ \rho vE + vp \end{pmatrix},$$

$$\mathbf{H}(\mathbf{Q}) = \begin{pmatrix} \rho uw \\ \rho vw \\ \rho w^2 + p \\ \rho w \\ \rho wE + wp \end{pmatrix}. \tag{3}$$

In general, the simplest form of the differential equations corresponds to nonconservative equations expressed in primitive variables, here taken as the set composed of velocity, pressure, and internal energy, $\mathbf{q} = (u, v, w, p, \epsilon)^T$. The primitive variables are related through the equation of state,

$$p = (\gamma - 1)\rho\epsilon, \tag{4}$$

$$\epsilon = E - \frac{1}{2}\left(u^2 + v^2 + w^2\right), \tag{5}$$

$$c^2 = \gamma p/\rho, \tag{6}$$

and γ is the ratio of specific heats.

The time-dependent nonconservative equations are found readily by transforming the time-dependent conservative equations.

$$\begin{aligned} \tfrac{\partial \mathbf{q}}{\partial \mathbf{Q}} \left[\partial_t \mathbf{Q} + \mathbf{R}\right] &= 0, \\ \partial_t \mathbf{q} + \tfrac{\partial \mathbf{q}}{\partial \mathbf{Q}} \mathbf{R} &= 0, \end{aligned} \tag{7}$$

where $\frac{\partial \mathbf{q}}{\partial \mathbf{Q}}$ is the Jacobian matrix of the transformation.

$$\frac{\partial \mathbf{q}}{\partial \mathbf{Q}} = \begin{pmatrix} 1/\rho & 0 & 0 & 0 & 0 \\ 0 & 1/\rho & 0 & 0 & 0 \\ 0 & 0 & 1/\rho & 0 & 0 \\ 0 & 0 & 0 & \gamma - 1 & 0 \\ 0 & 0 & 0 & 0 & 1/\rho \end{pmatrix} \begin{pmatrix} 1 & 0 & 0 & -u & 0 \\ 0 & 1 & 0 & -v & 0 \\ 0 & 0 & 1 & -w & 0 \\ -u & -v & -w & \frac{u^2+v^2+w^2}{2} & 1 \\ -u & -v & -w & -\epsilon + \frac{u^2+v^2+w^2}{2} & 1 \end{pmatrix} \tag{8}$$

For steady-state equations, the time derivative is dropped.

In an iterative procedure, the correction $\delta\mathbf{q} \equiv \mathbf{q}^{n+1} - \mathbf{q}^n$, where n is an iteration counter, can be computed from the equation

$$\mathbf{L}\,\delta\mathbf{q} = -\frac{\partial \mathbf{q}}{\partial \mathbf{Q}}\,\mathbf{R}, \tag{9}$$

where $\mathbf{L}$ is the principal linearization of the nonconservative operator.

$$\mathbf{L} = \begin{bmatrix} Q & 0 & 0 & \frac{1}{\rho}\partial_x & 0 \\ 0 & Q & 0 & \frac{1}{\rho}\partial_y & 0 \\ 0 & 0 & Q & \frac{1}{\rho}\partial_z & 0 \\ \rho c^2\partial_x & \rho c^2\partial_y & \rho c^2\partial_z & Q & 0 \\ \frac{c^2}{\gamma}\partial_x & \frac{c^2}{\gamma}\partial_y & \frac{c^2}{\gamma}\partial_z & 0 & Q \end{bmatrix}, \tag{10}$$

where $Q = \bar{u}\partial_x + \bar{v}\partial_y + \bar{w}\partial_z = (\mathbf{u}\cdot\nabla)$, and the coefficients $\mathbf{u} = (\bar{u}, \bar{v}, \bar{w})$, ρ, and c^2 are evaluated from the previous approximation $\mathbf{q}^n$ and, for the current iteration, are considered as known values unrelated to the target primitive variables. The last equation in (9) is decoupled from the first four, representing the convection of entropy along a streamline. The determinant of the matrix operator $\mathbf{L}$ is

$$Q^3\left[Q^2 - c^2\Delta\right], \tag{11}$$

where Δ is the Laplace operator, and $Q^2 - c^2\Delta$ represents the full-potential operator. Note that the right side of the correction equation (9) is a combination of conservative-discretization residuals. The left side approximates the nonconservative equations. Thus, away from discontinuities in the flow field, we expect a good correction to the previous solution approximation.

Distributed Relaxation: Differential Equations

The distributed relaxation method for the Euler equations replaces $\delta\mathbf{q}$ in (9) by $\mathbf{M}\delta\mathbf{w}$,

$$\mathbf{M} = \begin{bmatrix} 1 & 0 & 0 & -\frac{1}{\rho}\partial_x & 0 \\ 0 & 1 & 0 & -\frac{1}{\rho}\partial_y & 0 \\ 0 & 0 & 1 & -\frac{1}{\rho}\partial_z & 0 \\ 0 & 0 & 0 & Q & 0 \\ 0 & 0 & 0 & 0 & 1 \end{bmatrix}, \tag{12}$$

so that the resulting matrix $\mathbf{L}\,\mathbf{M}$ becomes lower triangular, as

$$\mathbf{L}\,\mathbf{M} = \begin{bmatrix} Q & 0 & 0 & 0 & 0 \\ 0 & Q & 0 & 0 & 0 \\ 0 & 0 & Q & 0 & 0 \\ \rho c^2\partial_x & \rho c^2\partial_y & \rho c^2\partial_z & Q^2 - c^2\Delta & 0 \\ \frac{c^2}{\gamma}\partial_x & \frac{c^2}{\gamma}\partial_y & \frac{c^2}{\gamma}\partial_z & 0 & Q \end{bmatrix}, \tag{13}$$

$$\mathbf{L}\,\mathbf{M}\,\delta\mathbf{w} = -\frac{\partial \mathbf{q}}{\partial \mathbf{Q}}\,\mathbf{R}. \tag{14}$$

The diagonal elements of $\mathbf{L}\,\mathbf{M}$ are composed of the factors of the matrix $\mathbf{L}$ determinant and represent the elliptic or hyperbolic partitions of the equation. The $\delta\mathbf{w}$ variables were termed earlier,[2,8] "ghost variables," because they need not explicitly appear in the calculations.

The distributed relaxation approach yields fast convergence for both steady and unsteady simulations, if the constituent scalar diagonal operators in $\mathbf{L}\,\mathbf{M}$ are solved with fast methods. The approach can be applied to quite general equations; a set of matrices $\mathbf{M}$ has been derived[2,3]) that provide a convenient lower triangular form for the compressible and incompressible equations of fluid dynamics (including a variable equation of state).

For the compressible Euler equations, the scalar factors constituting the main diagonal of $\mathbf{L}\,\mathbf{M}$ are convection and full-potential operators. An efficient solver for the former can be based on downstream marching, with additional special procedures for recirculating flows;[7,8,14,24] the latter is a variable type operator, and its solution requires different procedures in subsonic, transonic, and supersonic regions. In deep subsonic regions, the full-potential operator is uniformly elliptic and therefore standard multigrid methods yield optimal efficiency. When the Mach number approaches unity, the operator becomes increasingly anisotropic and, because some smooth characteristic error components cannot be approximated adequately on coarse grids, classical multigrid methods severely degrade. The characteristic components are those components that are much smoother in the characteristic directions than in other directions.[3,12,13] In the deep supersonic regions, the full-potential operator is uniformly hyperbolic with the stream direction serving as the time-like direction. In this region, an efficient solver can be obtained with a downstream marching method. However, downstream marching becomes problematic for the Mach number dropping towards unity, because the Courant number associated with this method becomes large. Thus, a special procedure is required to provide an efficient solution for transonic regions. A possible local procedure[4,5,10] is based on piecewise semicoarsening and some rules for adding dissipation at the coarse-grid levels.

Boundaries introduce some additional complexity in distributed relaxation. The determinant of $\mathbf{L}\,\mathbf{M}$ is usually higher order than the determinant of $\mathbf{L}$. In this case, it is higher by the factor Q. Thus, as a set of new variables, $\delta\mathbf{w}$ would generally need additional boundary conditions. In relaxation, because the ghost variables can be added in the external part of the domain, it is usually possible to determine suitable

boundary conditions for $\delta\mathbf{w}$ that satisfy the original boundary conditions for the primitive variables. Examples are given in[20] for incompressible flow with entering and no-slip boundaries. However, to construct such a remedy may be difficult and/or time-consuming in general. In addition, enforcing these boundary conditions causes the relaxation equations to be coupled near the boundaries, not decoupled as they are in the interior of the domain. Thus, near boundaries and discontinuities, the general approach[2,3] is to relax the governing equations directly in terms of primitive variables. Several sweeps of robust (but possibly slowly converging) relaxation, such as Newton-Kacmarcz relaxation, can be made in this region. The additional sweeps will not affect the overall complexity because the number of boundary and/or discontinuity points is usually negligible in comparison with the number of interior points.

Distributed Relaxation: Discrete Equations

The discrete equations are formulated in terms of discretized primitive variables. One way to attain a conservative finite-volume discretization, $\mathbf{R^h}$, corresponding to the discrete version of (1) requires an interpolation of the primitive variables to the interface locations, maintaining the required order of accuracy. In this paper, the considered grid is a Cartesian structured grid, although generalization to curvilinear coordinate systems is possible. At this moment, we do not make any assumptions about locations of the variables and volume interfaces, i.e., these locations can be staggered or collocated.

The equations for the relaxation update are formulated similarly to (9)

$$\mathbf{L^h}\,\delta\mathbf{q^h} = -\frac{\partial\mathbf{q}}{\partial\mathbf{Q}}\,\mathbf{R^h}. \tag{15}$$

The right side of the equations are a combination of the conservative residuals with the coefficients of $\frac{\partial\mathbf{q}}{\partial\mathbf{Q}}$ calculated at the points where the corresponding conservative equations are defined.

The derivation of the discrete operator $\mathbf{L^h}$ requires special considerations.

- The linear discrete operator $\mathbf{L^h}$ should relate to $\mathbf{R^h}$ as

$$\mathbf{L^h} = \frac{\partial\mathbf{q}}{\partial\mathbf{Q}}\,\mathcal{R}^h, \tag{16}$$

  where $\mathcal{R}^h$ is the principal linearization operator of $\mathbf{R^h}$.

- $\mathbf{L^h}$ should be factorizable.

- To reflect the correct domain of influence, the discrete factors appearing at the main diagonal of the matrix product $\mathbf{L^h}\,\mathbf{M^h}$, where $\mathbf{M^h}$ is the discrete distribution matrix (compare to (13)), should be type-dependent, i.e., central for elliptic factors and upwind (or upwind biased) for hyperbolic factors. For Euler equations, it is also required that the discretization of the full-potential factor reflects the physical anisotropies of the differential full-potential operator.

Some simplification can be achieved by replacing $\mathbf{L^h}$ with a less accurate operator providing a good convergence with defect-correction iterations. For staggered-grid nonconservative formulations, proper operators $\mathbf{L^h}$ have already been derived for incompressible and low-Mach-number flows.[1,2,19,20] For collocated-grid formulations, a family of factorizable discrete operators $\mathbf{L^h}$ is analyzed in.[11] The collocated-grid scheme presented in this paper belongs to this family. An alternative approach also resulting to factorizable discretizations is proposed by Sidilkover in[16,17]

The basic scheme, $\mathbf{L^h}_{\text{basic}}$, is similarly formulated for both staggered and collocated variable arrangements:

$$\mathbf{L^h}_{\text{basic}} = \begin{bmatrix} Q^h & 0 & 0 & \frac{1}{\rho}\partial_x^h & 0 \\ 0 & Q^h & 0 & \frac{1}{\rho}\partial_y^h & 0 \\ 0 & 0 & Q^h & \frac{1}{\rho}\partial_z^h & 0 \\ \rho c^2\partial_x^h & \rho c^2\partial_y^h & \rho c^2\partial_z^h & \bar{Q}^h & 0 \\ \frac{c^2}{\gamma}\partial_x^h & \frac{c^2}{\gamma}\partial_y^h & \frac{c^2}{\gamma}\partial_z^h & 0 & Q^h \end{bmatrix}, \tag{17}$$

where the discrete derivatives, $\partial_x^h, \partial_y^h, \partial_z^h$, in all off-diagonal terms are the second-order-accurate central-differencing approximation (short, i.e., with h-spacing for staggered grids and long, i.e., with $2h$-spacing, for collocated grids). All the diagonal terms, Q^h, except $\bar{Q}^h$ in the fourth equation, are discretized with the same second-order-accurate upwind (or upwind-biased) discretization scheme. In the subsonic regime ($|\mathbf{u}|^2 = \bar{u}^2 + \bar{v}^2 + \bar{w}^2 < c^2$), the $\bar{Q}^h$-term is differenced with a second-order-accurate downwind (or downwind-biased) discretization.

The determinant of the matrix operator $\mathbf{L^h}_{\text{basic}}$ is given by

$$\left(Q^h\right)^3\left[Q^h\bar{Q}^h - c^2\Delta^h\right], \tag{18}$$

where Δ is a discrete Laplace operator.

For staggered grids, the discrete full-potential operator appeared in the brackets is a reasonable h-elliptic operator. However, its stencil is somewhat wide (because of $Q^h\bar{Q}^h$) and does not reflect the physical anisotropies of the differential full-potential operator. The collocated-grid full-potential operator also has a wide stencil but suffers a more serious drawback: The Laplace operator Δ^h is a wide (with mesh spacing $2h$) operator. For slow velocities ($|\mathbf{u}| \approx 0$), the

discrete full-potential operator is dominated by this non-h-elliptic wide Laplacian; and efficiency of *any* local relaxation in error smoothing severely degrades.

A way to improve the discrete full-potential operator is to change the discretization of $\bar{Q}^h$ to $\bar{Q}^h + \mathcal{A}^h$. Then the discrete full-potential operator is changed to

$$Q^h \mathcal{A}^h + Q^h \bar{Q}^h - c^2 \Delta^h. \tag{19}$$

If the operator $\mathcal{A}^h$ is at least second-order small (proportional to h^2), the overall second-order discretization accuracy is not compromised. The ideal choice for $\mathcal{A}^h$ is $\mathcal{A}^h = \left(Q^h\right)^{-1} \mathcal{D}^h, \mathcal{D}^h = \mathcal{F}^h - (Q^h \bar{Q}^h - c^2 \Delta^h)$, where $\mathcal{F}^h$ is a desired discrete approximation for the full-potential factor. We omit the discussion on what would be the best discretization for the multidimensional subsonic full-potential operator. Note only that it is possible to construct a discretization that satisfies the following properties: (1) At low Mach numbers, the discretization is dominated by the standard (with mesh spacing h) h-elliptic Laplacian. (2) For the Mach number approaching unity, the discretization tends to the optimal discretization for the sonic-flow full-potential operator (see[4,5,10]).

The operator $\left(Q^h\right)^{-1}$ is a nonlocal operator and its introduction can be effected through a new auxiliary variable ψ^h and a new discrete equation $Q^h \psi^h = \mathcal{D}^h p^h$. For the purpose of constructing a corresponding conservative scheme, the new variable ψ^h should be further replaced with $\psi^h = Q^* \phi^h$, where Q^* is an arbitrary discrete approximation to the operator Q and ϕ^h is another auxiliary variable. Thus, the new vector of discrete unknowns becomes $\mathbf{q^h} = (u^h, v^h, w^h, \psi^h, p^h, \phi^h, \epsilon^h)^T$. The discrete operator $\mathbf{L^h}_{\text{basic}}$ is changed to $\mathbf{L^h}$

$$\mathbf{L^h} = \begin{bmatrix} Q^h & 0 & 0 & 0 & \frac{1}{\rho}\partial_x^h & 0 & 0 \\ 0 & Q^h & 0 & 0 & \frac{1}{\rho}\partial_y^h & 0 & 0 \\ 0 & 0 & Q^h & 0 & \frac{1}{\rho}\partial_z^h & 0 & 0 \\ 0 & 0 & 0 & Q^h & -\mathcal{D}^h & 0 & 0 \\ \rho c^2 \partial_x^h & \rho c^2 \partial_y^h & \rho c^2 \partial_z^h & 1 & \bar{Q}^h & 0 & 0 \\ 0 & 0 & 0 & -1 & 0 & Q^* & 0 \\ \frac{c^2}{\gamma}\partial_x^h & \frac{c^2}{\gamma}\partial_y^h & \frac{c^2}{\gamma}\partial_z^h & 0 & 0 & 0 & Q^h \end{bmatrix}. \tag{20}$$

The corresponding distribution matrix, $\mathbf{M^h}$, for distributed relaxation is defined as

$$\mathbf{M^h} = \begin{bmatrix} 1 & 0 & 0 & 0 & -\frac{1}{\rho}\partial_x^h & 0 & 0 \\ 0 & 1 & 0 & 0 & -\frac{1}{\rho}\partial_y^h & 0 & 0 \\ 0 & 0 & 1 & 0 & -\frac{1}{\rho}\partial_z^h & 0 & 0 \\ 0 & 0 & 0 & 1 & \mathcal{D}^h & 0 & 0 \\ 0 & 0 & 0 & 0 & Q^h & 0 & 0 \\ 0 & 0 & 0 & 0 & 0 & 1 & 0 \\ 0 & 0 & 0 & 0 & 0 & 0 & 1 \end{bmatrix}, \tag{21}$$

so that the resulting matrix $\mathbf{L^h}\,\mathbf{M^h}$ becomes lower triangular as

$$\mathbf{L^h}\,\mathbf{M^h} = \begin{bmatrix} Q^h & 0 & 0 & 0 & 0 & 0 & 0 \\ 0 & Q^h & 0 & 0 & 0 & 0 & 0 \\ 0 & 0 & Q^h & 0 & 0 & 0 & 0 \\ 0 & 0 & 0 & Q^h & 0 & 0 & 0 \\ \rho c^2 \partial_x^h & \rho c^2 \partial_y^h & \rho c^2 \partial_z^h & 1 & \mathcal{F}^h & 0 & 0 \\ 0 & 0 & 0 & -1 & 0 & Q^* & 0 \\ \frac{c^2}{\gamma}\partial_x^h & \frac{c^2}{\gamma}\partial_y^h & \frac{c^2}{\gamma}\partial_z^h & 0 & 0 & 0 & Q^h \end{bmatrix}. \tag{22}$$

In the following sections, a direct correspondence between the primitive variable interpolations for calculating fluxes in the conservative discretization and stencils of the discretized derivatives in the nonconservative formulation is established. This correspondence can be used in several ways. For example, one can define interpolations of variables in a conservative discretization so that the corresponding operator $\mathbf{L^h}$ from (16) coincides with a predefined linear operator derived from a nonconservative formulation. As another example, one can derive the linear operator $\mathbf{L^h}$ corresponding to a given conservative discretization and then try to find an appropriate matrix $\mathbf{M^h}$ to design an efficient distributed relaxation. Some mixed requirements, partially defined by the interpolations in the conservative discretization and partially by the discretization stencils in $\mathbf{L^h}$, are also possible.

A brief description of the derivation of the conservative-nonconservative correspondence can be done as follows. The starting point is the full Newton linearization of the conservative discretization. This linear operator acts on the perturbation function. The assumption of smoothness suggests that the changes of primitive variables on the scale of the characteristic meshsize are small in comparison with the absolute value of the function. Under this assumption the principal linearization, $\mathcal{R}^h$, retains only terms including the perturbation function derivatives rather than the perturbation function itself. The product $\frac{\partial \mathbf{q}}{\partial \mathbf{Q}}\,\mathcal{R}^h$ approximates the set of nonconservative equations; and one can use it to establish the relations between the flux interpolations in the conservative discretization and the discrete differencing in $\mathbf{L^h}$.

In addition to regions with shocks and slip lines, the smoothness assumption is not valid in the regions where primitive variables have small absolute values, e.g., in the neighborhood of a stagnation point; in these regions, therefore, distributed relaxation should be replaced with local relaxation.

One-Dimensional Euler System

The steady-state one-dimensional equations express the conservation of momentum, mass, and total energy as

$$\mathbf{R}(\mathbf{Q}) = 0, \tag{23}$$

where

$$\mathbf{Q} \equiv (\rho u, \rho, \rho E)^T, \tag{24}$$
$$\mathbf{R} \equiv \partial_x(\mathbf{F}). \tag{25}$$

The flux $\mathbf{F}$ is defined as

$$\mathbf{F} \equiv \begin{pmatrix} \rho u^2 + p \\ \rho u \\ \rho u E + up \end{pmatrix}, \tag{26}$$

The vector of primitive variables is $\mathbf{q} = (u, p, \epsilon)^T$. The Jacobian matrix of the conservative-to-nonconservative transformation is defined as

$$\frac{\partial \mathbf{q}}{\partial \mathbf{Q}} = \begin{pmatrix} \frac{1}{\rho} & 0 & 0 \\ 0 & (\gamma-1) & 0 \\ 0 & 0 & \frac{1}{\rho} \end{pmatrix} \begin{pmatrix} 1 & -u & 0 \\ -u & \frac{u^2}{2} & 1 \\ -u & -\epsilon + \frac{u^2}{2} & 1 \end{pmatrix}. \tag{27}$$

The set of the nonconservative equations is defined as

$$\begin{pmatrix} u\partial_x & \frac{(\gamma-1)\epsilon}{p}\partial_x & 0 \\ \gamma p \partial_x & u\partial_x & 0 \\ (\gamma-1)\epsilon\partial_x & 0 & u\partial_x \end{pmatrix} \begin{pmatrix} u \\ p \\ \epsilon \end{pmatrix} = 0. \tag{28}$$

The discrete matrix operator corresponding to (28) is defined as

$$\begin{pmatrix} u\breve{D}^u & \frac{(\gamma-1)\epsilon}{p}\breve{D}^p & \breve{\mathcal{D}}^\epsilon \\ \gamma p \bar{D}^u & u\bar{D}^p & \frac{up}{\epsilon}\bar{\mathcal{D}}^\epsilon \\ (\gamma-1)\epsilon\hat{D}^u & \frac{u\epsilon}{p}\hat{\mathcal{D}}^p & u\hat{D}^\epsilon \end{pmatrix}, \tag{29}$$

where the D-entries are some discrete operators approximating the first derivatives from (28); the $\mathcal{D}$-entries approximate zeros, meaning that the difference operators can either be zeros or approximate a higher order derivative multiplied by a power of h; the superscript denotes the variable to which the difference operator is applied. In most cases, the operators are computed at integer locations except for staggered arrangements, where the *breve* operators are defined at half-integer locations.

The conservative discretization of $\mathbf{R}$ (23) can be explicitly written out as

$$\mathbf{R}^{\mathbf{h}} = \frac{1}{h}\begin{pmatrix} \frac{\breve{P}_{\text{right}}\breve{U}^2_{\text{right}}}{(\gamma-1)\breve{E}_{\text{right}}} + \breve{P}_{\text{right}} \\ \frac{\bar{P}_{\text{right}}\bar{U}_{\text{right}}}{(\gamma-1)\bar{E}_{\text{right}}} \\ \frac{\hat{P}_{\text{right}}\hat{U}_{\text{right}}}{(\gamma-1)\hat{E}_{\text{right}}}\left(\gamma\hat{E}_{\text{right}} + \frac{\hat{U}^2_{\text{right}}}{2}\right) \end{pmatrix} - \frac{1}{h}\begin{pmatrix} \frac{\breve{P}_{\text{left}}\breve{U}^2_{\text{left}}}{(\gamma-1)\breve{E}_{\text{left}}} + \breve{P}_{\text{left}} \\ \frac{\bar{P}_{\text{left}}\bar{U}_{\text{left}}}{(\gamma-1)\bar{E}_{\text{left}}} \\ \frac{\hat{P}_{\text{left}}\hat{U}_{\text{left}}}{(\gamma-1)\hat{E}_{\text{left}}}\left(\gamma\hat{E}_{\text{left}} + \frac{\hat{U}^2_{\text{left}}}{2}\right) \end{pmatrix}, \tag{30}$$

where the capital letters designate the interpolations of the primitive variables to the flux locations (E representing interpolation of ϵ). Note that these interpolations can be different for different equations, therefore, breve, bar, and hat notations for momentum, mass, and energy conservation equations respectively. Under the smoothness assumption, the principal linearization $\mathcal{R}^h$ of $\mathbf{R}^{\mathbf{h}}$ applied to disturbance function, $\delta\mathbf{q}$, results in a set of the three linear operators.

$$\begin{aligned} \breve{\mathcal{R}}^h(\delta\mathbf{q}) &\equiv \frac{2\tilde{P}\tilde{U}}{(\gamma-1)\tilde{E}}\frac{(\breve{\delta u})_{\text{right}} - (\breve{\delta u})_{\text{left}}}{h} \\ &\quad + \left(1 + \frac{\tilde{U}^2}{(\gamma-1)\tilde{E}}\right)\frac{(\breve{\delta p})_{\text{right}} - (\breve{\delta p})_{\text{left}}}{h} \\ &\quad - \frac{\breve{P}\tilde{U}^2}{(\gamma-1)\tilde{E}^2}\frac{(\breve{\delta\epsilon})_{\text{right}} - (\breve{\delta\epsilon})_{\text{left}}}{h} \\ &\equiv \frac{2\tilde{P}\tilde{U}}{(\gamma-1)\tilde{E}}\breve{\Delta}^u + \left(1 + \frac{\tilde{U}^2}{(\gamma-1)\tilde{E}}\right)\breve{\Delta}^p - \frac{\tilde{P}\tilde{U}^2}{(\gamma-1)\tilde{E}^2}\breve{\Delta}^\epsilon, \end{aligned}$$

$$\begin{aligned} \bar{\mathcal{R}}^h(\delta\mathbf{q}) &\equiv \frac{\tilde{P}}{(\gamma-1)\tilde{E}}\frac{(\bar{\delta u})_{\text{right}} - (\bar{\delta u})_{\text{left}}}{h} \\ &\quad + \frac{\tilde{U}}{(\gamma-1)\tilde{E}}\frac{(\bar{\delta p})_{\text{right}} - (\bar{\delta p})_{\text{left}}}{h} \\ &\quad - \frac{\tilde{P}\tilde{U}}{(\gamma-1)\tilde{E}^2}\frac{(\bar{\delta\epsilon})_{\text{right}} - (\bar{\delta\epsilon})_{\text{left}}}{h} \\ &\equiv \frac{\tilde{P}}{(\gamma-1)\tilde{E}}\bar{\Delta}^u + \frac{\tilde{U}}{(\gamma-1)\tilde{E}}\bar{\Delta}^p - \frac{\tilde{P}\tilde{U}}{(\gamma-1)\tilde{E}^2}\bar{\Delta}^\epsilon, \end{aligned}$$

$$\hat{\mathcal{R}}^h(\delta\mathbf{q}) \equiv \left(\frac{\gamma\tilde{P}}{\gamma-1}+\frac{3\tilde{P}\tilde{U}^2}{2(\gamma-1)\tilde{E}}\right)\frac{(\hat{\delta u})_{\text{right}}-(\hat{\delta u})_{\text{left}}}{h} + \frac{\tilde{U}\left(\gamma\tilde{E}+\frac{\tilde{U}^2}{2}\right)}{(\gamma-1)\tilde{E}}\frac{(\hat{\delta p})_{\text{right}}-(\hat{\delta p})_{\text{left}}}{h} - \frac{\tilde{P}\tilde{U}^3}{2(\gamma-1)\tilde{E}^2}\frac{(\hat{\delta\epsilon})_{\text{right}}-(\hat{\delta\epsilon})_{\text{left}}}{h}$$

$$\equiv \left(\frac{\gamma\tilde{P}}{\gamma-1}+\frac{3\tilde{P}\tilde{U}^2}{2(\gamma-1)\tilde{E}}\right)\hat{\Delta}^u + \frac{\tilde{U}\left(\gamma\tilde{E}+\frac{\tilde{U}^2}{2}\right)}{(\gamma-1)\tilde{E}}\hat{\Delta}^p - \frac{\tilde{P}\tilde{U}^3}{2(\gamma-1)\tilde{E}^2}\hat{\Delta}^\epsilon,$$

where the $\mathcal{R}^h$ operators are defined at the same locations as the corresponding operators in (28), i.e., for collocated grids – at integer points, for staggered grids – the first operator, $\breve{\mathcal{R}}^h$, is defined at half-integer points. Tilde values are arbitrary interpolations satisfying the desired accuracy order, and the Δ-notation is self-explanatory.

Using (27), an approximation to the first equation of (28) is obtained as

$$\frac{(\gamma-1)\tilde{E}}{\tilde{P}}\left(\breve{\mathcal{R}}^h-\tilde{U}\bar{\mathcal{R}}^h\right) \equiv \tilde{U}\left(2\breve{\Delta}^u-\bar{\Delta}^u\right) + \frac{(\gamma-1)\tilde{E}}{\tilde{P}}\Delta^p + \frac{\tilde{U}^2}{\tilde{P}}\left(\breve{\Delta}^p-\bar{\Delta}^p\right) - \frac{\tilde{U}^2}{\tilde{E}}\left(\breve{\Delta}^\epsilon-\bar{\Delta}^\epsilon\right) \quad (31)$$

For staggered grids, the bar-operators ($\bar{\mathcal{R}}^h, \bar{\Delta}^u, \bar{\Delta}^p$, and $\bar{\Delta}^\epsilon$) are averaged from the neighboring locations. Approximations to the second and third equations of (28) are similarly computed:

$$\begin{aligned}&(\gamma-1)\left(-\tilde{U}\breve{\mathcal{R}}^h+\tfrac{\tilde{U}^2}{2}\bar{\mathcal{R}}^h+\hat{\mathcal{R}}^h\right)\equiv\\ &\gamma\tilde{P}\hat{\Delta}^u+\tfrac{\tilde{U}^2\tilde{P}}{\tilde{E}}\left(-2\breve{\Delta}^u+\tfrac{1}{2}\bar{\Delta}^u+\tfrac{3}{2}\hat{\Delta}^u\right)\\ &+\tilde{U}\left(\gamma\hat{\Delta}^p-(\gamma-1)\breve{\Delta}^p\right)+\tfrac{\tilde{U}^3}{\tilde{E}}\left(-\breve{\Delta}^p+\tfrac{1}{2}\bar{\Delta}^p+\tfrac{1}{2}\hat{\Delta}^p\right)\\ &+\tfrac{\tilde{P}\tilde{U}^3}{\tilde{E}^2}\left(\breve{\Delta}^\epsilon-\tfrac{1}{2}\bar{\Delta}^\epsilon-\tfrac{1}{2}\hat{\Delta}^\epsilon\right),\end{aligned} \quad (32)$$

$$\begin{aligned}&\tfrac{(\gamma-1)\tilde{E}}{\tilde{P}}\left(-\tilde{U}\breve{\mathcal{R}}^h+\left(-\tilde{E}+\tfrac{\tilde{U}^2}{2}\right)\bar{\mathcal{R}}^h+\hat{\mathcal{R}}^h\right)\equiv\\ &\tilde{E}\left(-\bar{\Delta}^u+\gamma\hat{\Delta}^u\right)+\tilde{U}^2\left(-2\breve{\Delta}^u+\tfrac{1}{2}\bar{\Delta}^u+\tfrac{3}{2}\hat{\Delta}^u\right)\\ &+\tfrac{(\gamma-1)\tilde{U}\tilde{E}}{\tilde{P}}\left(-\breve{\Delta}^p-\tfrac{1}{\gamma-1}\bar{\Delta}^p+\tfrac{\gamma}{\gamma-1}\hat{\Delta}^p\right)\\ &+\tfrac{\tilde{U}^3}{\tilde{P}}\left(-\breve{\Delta}^p+\tfrac{1}{2}\bar{\Delta}^p+\tfrac{1}{2}\hat{\Delta}^p\right)\\ &+\tilde{U}\bar{\Delta}^\epsilon+\tfrac{\tilde{U}^3}{\tilde{E}}\left(\breve{\Delta}^\epsilon-\tfrac{1}{2}\bar{\Delta}^\epsilon-\tfrac{1}{2}\hat{\Delta}^\epsilon\right).\end{aligned} \quad (33)$$

For staggered-grid formulation, breve-values are computed as averages of corresponding values at the half-integer points.

Comparison of (31)–(33) with (29) gives the following relations between conservative and nonconservative discretizations. The recurrent representation form is chosen for the sake of compactness.

$$\bar{\Delta}^u=\gamma\bar{D}^u-(\gamma-1)\hat{D}^u, \quad (34)$$

$$\breve{\Delta}^u=\frac{1}{2}\breve{D}^u+\frac{1}{2}\bar{\Delta}^u, \quad (35)$$

$$\hat{\Delta}^u=\vartheta\left(\bar{D}^u-\beta\left(-2\breve{\Delta}^u+\frac{1}{2}\bar{\Delta}^u\right)\right), \quad (36)$$

$$\bar{\Delta}^p=\bar{D}^p-\hat{\mathcal{D}}^p, \quad (37)$$

$$\breve{\Delta}^p=\frac{1}{1+\gamma M^2}\left(\breve{D}^p+\gamma M^2\bar{\Delta}^p\right), \quad (38)$$

$$\hat{\Delta}^p=\theta\left(\frac{1}{\gamma}\bar{D}^p+\left(\frac{\gamma-1}{\gamma}+\beta\right)\breve{\Delta}^p-\beta\frac{1}{2}\bar{\Delta}^p\right) \quad (39)$$

$$\bar{\Delta}^\epsilon=\hat{D}^\epsilon-\bar{\mathcal{D}}^\epsilon, \quad (40)$$

$$\breve{\Delta}^\epsilon=-\frac{2}{\gamma\beta}\breve{\mathcal{D}}^\epsilon+\bar{\Delta}^\epsilon, \quad (41)$$

$$\hat{\Delta}^\epsilon=\frac{2}{\gamma\beta}\left(\bar{\mathcal{D}}^\epsilon-\gamma\beta\left(\breve{\Delta}^\epsilon-\frac{1}{2}\bar{\Delta}^\epsilon\right)\right), \quad (42)$$

where $M^2=u^2/c^2=u^2/(\gamma(\gamma-1)\epsilon)$ is the local (squared) Mach number at the point defined by the subscript index j, $\beta\equiv(\gamma-1)M^2$, $\theta\equiv\frac{1}{1+\frac{1}{2}\beta}$, and $\vartheta\equiv\frac{1}{1+\frac{3}{2}\beta}$.

Derivation of the conservative discretization corresponding to a given nonconservative scheme

Let us consider three different discretizations of (29) associated with the subsonic flow regime. In all the cases the $\mathcal{D}$-entries are zeros and other off-diagonal terms are second-order accurate central discretizations of the first derivative.

A *First-order scheme:* $\breve{D}^u$ and $\hat{D}^\epsilon$ are the first-order upwind discretizations, $\bar{D}^p$ is the first-order downwind discretization.

B *Second-order biased scheme:* $\breve{D}^u$ and $\hat{D}^\epsilon$ are the second-order upwind discretizations, $\bar{D}^p$ is the second-order downwind discretization.

C *Second-order central scheme:* $\breve{D}^u$, $\hat{D}^\epsilon$, and $\bar{D}^p_j$ are the second-order central discretizations.

The following formulas define the interpolations for evaluating fluxes in the conservative discretization (30); the superscript NC denotes the fluxes in representation of the D-derivative terms of (29) (see Table 1.)

Table 1 The fluxes in representation of the D-derivative terms of (29).

	A	B	C
$\breve{D}_j^u = \frac{\breve{U}^{NC}_{j+\frac{1}{2}} - \breve{U}^{NC}_{j-\frac{1}{2}}}{h}$	$\breve{D}_j^u = \frac{u_j - u_{j-1}}{h}$ $\breve{U}^{NC}_{j+\frac{1}{2}} = u_j$	$\breve{D}_j^u = \frac{\frac{3}{2}u_j - 2u_{j-1} + \frac{1}{2}u_{j-2}}{h}$ $\breve{U}^{NC}_{j+\frac{1}{2}} = \frac{3}{2}u_j - \frac{1}{2}u_{j-1}$	$\breve{D}_j^u = \frac{u_{j+1} - u_{j-1}}{2h}$ $\breve{U}^{NC}_{j+\frac{1}{2}} = \frac{1}{2}u_{j+1} + \frac{1}{2}u_j$
$\breve{D}_j^p = \frac{\breve{P}^{NC}_{j+\frac{1}{2}} - \breve{P}^{NC}_{j-\frac{1}{2}}}{h}$	$\breve{D}_j^p = \frac{p_{j+1} - p_{j-1}}{2h}$ $\breve{P}^{NC}_{j+\frac{1}{2}} = \frac{1}{2}p_{j+1} + \frac{1}{2}p_j$	$\breve{D}_j^p = \frac{p_{j+1} - p_{j-1}}{2h}$ $\breve{P}^{NC}_{j+\frac{1}{2}} = \frac{1}{2}p_{j+1} + \frac{1}{2}p_j$	$\breve{D}_j^p = \frac{p_{j+1} - p_{j-1}}{2h}$ $\breve{P}^{NC}_{j+\frac{1}{2}} = \frac{1}{2}p_{j+1} + \frac{1}{2}p_j$
$\bar{D}_j^u = \frac{\bar{U}^{NC}_{j+\frac{1}{2}} - \bar{U}^{NC}_{j-\frac{1}{2}}}{h}$	$\bar{D}_j^u = \frac{u_{j+1} - u_{j-1}}{2h}$ $\bar{U}^{NC}_{j+\frac{1}{2}} = \frac{1}{2}u_{j+1} + \frac{1}{2}u_j$	$\bar{D}_j^u = \frac{u_{j+1} - u_{j-1}}{2h}$ $\bar{U}^{NC}_{j+\frac{1}{2}} = \frac{1}{2}u_{j+1} + \frac{1}{2}u_j$	$\bar{D}_j^u = \frac{u_{j+1} - u_{j-1}}{2h}$ $\bar{U}^{NC}_{j+\frac{1}{2}} = \frac{1}{2}u_{j+1} + \frac{1}{2}u_j$
$\bar{D}_j^p = \frac{\bar{P}^{NC}_{j+\frac{1}{2}} - \bar{P}^{NC}_{j-\frac{1}{2}}}{h}$	$\bar{D}_j^p = \frac{p_{j+1} - p_j}{h}$ $\bar{P}^{NC}_{j+\frac{1}{2}} = p_{j+1}$	$\bar{D}_j^p = \frac{-\frac{1}{2}p_{j+2} + 2p_{j+1} - \frac{3}{2}p_j}{h}$ $\bar{P}^{NC}_{j+\frac{1}{2}} = \frac{3}{2}p_{j+1} - \frac{1}{2}p_{j+2}$	$\bar{D}_j^p = \frac{p_{j+1} - p_{j-1}}{2h}$ $\bar{P}^{NC}_{j+\frac{1}{2}} = \frac{1}{2}p_j + \frac{1}{2}p_{j+1}$
$\hat{D}_j^u = \frac{\hat{U}^{NC}_{j+\frac{1}{2}} - \hat{U}^{NC}_{j-\frac{1}{2}}}{h}$	$\hat{D}_j^u = \frac{u_{j+1} - u_{j-1}}{2h}$ $\hat{U}^{NC}_{j+\frac{1}{2}} = \frac{1}{2}u_{j+1} + \frac{1}{2}u_j$	$\hat{D}_j^u = \frac{u_{j+1} - u_{j-1}}{2h}$ $\hat{U}^{NC}_{j+\frac{1}{2}} = \frac{1}{2}u_{j+1} + \frac{1}{2}u_j$	$\hat{D}_j^u = \frac{u_{j+1} - u_{j-1}}{2h}$ $\hat{U}^{NC}_{j+\frac{1}{2}} = \frac{1}{2}u_{j+1} + \frac{1}{2}u_j$
$\hat{D}_j^\epsilon = \frac{\hat{E}^{NC}_{j+\frac{1}{2}} - \hat{E}^{NC}_{j-\frac{1}{2}}}{h}$	$\hat{D}_j^\epsilon = \frac{\epsilon_j - \epsilon_{j-1}}{h}$ $\hat{E}^{NC}_{j+\frac{1}{2}} = \epsilon_j$	$\hat{D}_j^\epsilon = \frac{\frac{3}{2}\epsilon_j - 2\epsilon_{j-1} + \frac{1}{2}\epsilon_{j-2}}{h}$ $\hat{E}^{NC}_{j+\frac{1}{2}} = \frac{3}{2}\epsilon_j - \frac{1}{2}\epsilon_{j-1}$	$\hat{D}_j^\epsilon = \frac{\epsilon_{j+1} - \epsilon_{j-1}}{2h}$ $\hat{E}^{NC}_{j+\frac{1}{2}} = \frac{1}{2}\epsilon_j + \frac{1}{2}\epsilon_{j+1}$

$$\bar{U}_{j+\frac{1}{2}} = \gamma \bar{U}^{NC}_{j+\frac{1}{2}} + (1-\gamma)\hat{U}^{NC}_{j+\frac{1}{2}}, \tag{43}$$

$$\breve{U}_{j+\frac{1}{2}} = \frac{1}{2}\breve{U}^{NC}_{j+\frac{1}{2}} + \frac{1}{2}\bar{U}_{j+\frac{1}{2}}, \tag{44}$$

$$\hat{U}_{j+\frac{1}{2}} = \vartheta\left[\bar{U}^{NC}_{j+\frac{1}{2}} - \beta\left(-2\breve{U}_{j+\frac{1}{2}} + \frac{1}{2}\bar{U}_{j+\frac{1}{2}}\right)\right] \tag{45}$$

$$\bar{P}_{j+\frac{1}{2}} = \bar{P}^{NC}_{j+\frac{1}{2}}, \tag{46}$$

$$\breve{P}_{j+\frac{1}{2}} = \frac{1}{1+\gamma M^2}\left(\breve{P}^{NC}_{j+\frac{1}{2}} + \gamma M^2 \bar{P}_{j+\frac{1}{2}}\right), \tag{47}$$

$$\hat{P}_{j+\frac{1}{2}} = \zeta\left[\bar{P}^{NC}_{j+\frac{1}{2}} - \gamma\beta\bar{P}_{j+\frac{1}{2}}\right] + \zeta(\gamma-1)\left(1 + \gamma M^2_{j+\frac{1}{2}}\breve{P}_{j+\frac{1}{2}}\right) \tag{48}$$

$$\bar{E}_{j+\frac{1}{2}} = \hat{E}^{NC}_{j+\frac{1}{2}}, \tag{49}$$

$$\breve{E}_{j+\frac{1}{2}} = \bar{E}_{j+\frac{1}{2}}, \tag{50}$$

$$\hat{E}_{j+\frac{1}{2}} = \bar{E}_{j+\frac{1}{2}} \tag{51}$$

where $\zeta \equiv \frac{1}{\gamma + \frac{1}{2}\gamma\beta}$.

Details of a collocated-grid scheme

The flux computations for a collocated-grid scheme can be constructed more simply by separating the mass flux contributions in each equation. Using the definitions in Table 1, the flux contributions at the interface locations $j+\frac{1}{2}$ are given below.

$$(\rho u) = \frac{\bar{P}^{NC}\bar{U}^{NC}}{(\gamma-1)\hat{E}^{NC}}, \tag{52}$$

$$(\rho u^2 + p) = (\rho u)\breve{U}^{NC} + \breve{P}^{NC}, \tag{53}$$

$$(\rho u E + p u) = (\rho u)\hat{E}^{NC} + \breve{P}^{NC}\bar{U}^{NC}. \tag{54}$$

The factor ϕ is introduced into the mass flux so the scheme remains conservative, as

$$\hat{\phi}^{NC}_{j+\frac{1}{2}} = \frac{3}{2}\phi j - \frac{1}{2}\phi_{j-1}. \tag{55}$$

where the fully-upwind scheme is used and Q^* is taken as Q. Since ϕ is second order small, zero conditions are imposed at the boundaries.

Numerical Tests

Computational results are shown in this section for the quasi-one-dimensional Euler equations. A uniform grid of N points is used over the domain $0 \le x \le 1$ with $h = 1/(N-1)$. The area distribution is defined as $\sigma(x) = 1 - 0.8x(1-x)$. The flow is fully subsonic and the inflow Mach number is 0.5. For all of the results presented below, we overspecify values from the exact solution of the differential problem at the boundary and at locations outside the domain; hence conservative fluxes are established at the half-grid locations surrounding the interior points.

The maximum discretization errors versus grid size in Fig. 1 shows a second-order spatial convergence. The results were converged using a Full Multigrid (FMG) cycle starting from a converged solution for $h = 1/16$ and using two relaxations of a nonconservative operator, Eq. (15), at each subsequent level. In Table 2, the L_2-norm of the discretization error in pressure, $e_d \equiv p_j - p(x_j)^{exact}$, corresponds to the results with zero algebraic erors. The ratios of the algebraic error in this L_2-norm to the discretization error in this norm for the FMG cycle are quite small at each grid. Because the nonconservative operator is factorizable and distributed relaxation has been demonstrated previously to be efficient solvers for nonconservative discretizations, we infer that distributed relaxation would yield high efficiency for this conservative discretization. It remains to demonstrate this for more

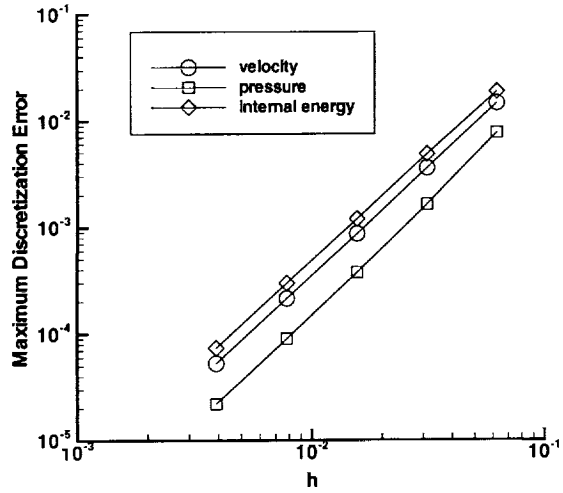

Fig. 1 Maximum discretization errors versus grid size for model problem.

h	$\|\|e_d\|\| : p$	$\|\|e_a\|\|/\|\|e_d\|\| : p$
1/32	$0.7323\text{x}10^{-3}$	0.043
1/64	$0.1618\text{x}10^{-3}$	0.086
1/128	$0.3856\text{x}10^{-4}$	0.006
1/256	$0.9447\text{x}10^{-5}$	0.004

Table 2 The L_2-norm of errors in p at convergence and the ratio of algebraic-to-discretization errors after an FMG cycle with two nonconservative relaxations on each grid.

general situations, including applications with more general boundary conditions and to flows with captured shocks.

Concluding Remarks

This paper has provided some foundations for the application of distributed relaxation to conservative discretizations. A direct correspondence between the primitive variable interpolations for calculating fluxes in conservative finite-volume discretizations and stencils of the discretized derivatives in the nonconservative formulation has been established. Based on this correspondence, one can design a conservative discretization which is very efficiently solved with a nonconservative relaxation scheme. This has been demonstrated for a conservative discretization of the quasi one-dimensional Euler equations on a collocated grid. Formulations for both staggered and collocated grid arrangements as well as extensions of the general procedure to multiple dimensions have been discussed.

References

[1]A. BRANDT, *Guide to multigrid development*, in Multigrid Methods, W. Hackbusch and U. Trottenberg, eds., Lecture Notes in Math. 960, Springer-Verlag, Berlin, 1982.

[2]———, *Multigrid techniques: 1984 guide with applications to fluid dynamics*, in Lecture Notes for the Computational Fluid Dynamics, Lecture Series at the Von-Karman Institute for Fluid Dynamics, The Weizmann Institute of Science, Rehovot, Israel, 1984. ISBN-3-88457-081-1, GMD-Studien Nr. 85, Available from GMD-AIW, Postfach 1316, D-53731, St. Augustin 1, Germany. Also available from Secretary, Department of Mathematics, University of Colorado at Denver, CO 80204-5300.

[3]———, *Barriers to achieving textbook multigrid efficiency in CFD*, ICASE Interim Report 32, NASA CR-1998-207647, April 1998. Updated version available as Gauss Center Report WI/GC-10 at The Weizmann Institute of Science, Rehovot, Israel, December 1998.

[4]A. BRANDT AND B. DISKIN, *Multigrid solvers for the nonaligned sonic flow: The constant coefficient case*, Computers and Fluids, 28 (1999), pp. 511–549. Also Gauss Center Report WI/GC-8 at The Weizmann Institute of Science, Rehovot, Israel, October 1997.

[5]———, *Multigrid solvers for nonaligned sonic flows*, SIAM J. Sci. Comp., 21 (2000), pp. 473–501.

[6]A. BRANDT, B. DISKIN, AND J. L. THOMAS, *Textbook multigrid efficiency for computational fluid dynamics simulations*, AIAA Paper 2001-2570, 15th AIAA CFD Conference, Anaheim, CA, June 2001.

[7]A. BRANDT AND I. YAVNEH, *On multigrid solution of high-Reynolds incompressible entering flow*, J. Comput. Phys., 101 (1992), pp. 151–164.

[8]———, *Accelerated multigrid convergence and high-Reynolds recirculating flows*, SIAM J. Sci. Comp., 14 (1993), pp. 607–626.

[9]W. L. BRIGGS, S. F. MCCORMICK, AND V. E.HENSON, *Multigrid Tutorial, 2nd edition*, SIAM, USA, 2000.

[10]B. DISKIN, *Efficient Multigrid Solvers for the Linearaized Transonic Full Potential Equation*, PhD thesis, The Weizmann Institute of Science, 1998.

[11]B. DISKIN AND J. L. THOMAS, *One-dimensional analysis of a factorizable h-elliptic discretization of the Euler equations.* (in preparation).

[12]———, *Solving upwind-biased discretizations: Defect-correction iterations*, ICASE Report 99-14, NASA CR-1999-209106, March 1999.

[13]———, *Half-space analysis of the defect-correction method for Fromm discretization of convection*, SIAM J. Sci. Comp., 22 (2000), pp. 633–655.

[14]C. W. OOSTERLEE AND T. WASHIO, *Krylov subspace acceleration of nonlinear multigrid with application to recirculating flows*, SIAM J. Scient. Comp., 21(5) (2000), pp. 1670–1690.

[15]P. L. ROE, *Approximate Riemann solvers, parameter vectors, and difference schemes*, J. Comp. Phys., 43 (1981), pp. 357–72.

[16]D. SIDILKOVER, *Factorizable scheme for the equation of fluid flow*, ICASE Report 99-20, NASA CR-1999-209345, June 1999.

[17]———, *Some approaches toward constructing optimally efficient multigrid solvers for the inviscid flow equations*, Computers and Fluids, 28 (1999), pp. 551–571.

[18]K. STÜBEN AND U. TROTTENBERG, *Multigrid methods: Fundamental algorithms, model problem analysis and application*, in Multigrid Methods, W. Hackbusch and U. Trottenberg, eds., Lecture Notes in Math. 960, Springer-Verlag, Berlin, 1982, pp. 1–176.

[19]J. L. THOMAS, B. DISKIN, AND A. BRANDT, *Distributed relaxation multigrid and defect correction applied to the compressible Navier-Stokes equations*, AIAA Paper 99-3334, 14th Computational Fluid Dynamics Conference, Norfolk, VA, July 1999.

[20]———, *Textbook multigrid efficiency for the incompressible Navier-Stokes equations: High Reynolds number wakes and boundary layers*, ICASE Report 99-51, NASA CR-1999-209831, December 1999. To appear in *Computers and Fluids.*

[21]J. L. THOMAS, B. DISKIN, A. BRANDT, AND J. C. SOUTH, *General framework for achieving textbook multigrid efficiency:*

Quasi-1-d Euler example, in Frontiers of Computational Fluid Dynamics — 2000, D. A. Caughey and M. M. Hafez, eds., Half Moon Bay, California, June 2000, World Scientific Publishing Company pte. ltd. Also ICASE Report 2000-30, NASA/CR-2000-210320.

[22]U. TROTTENBERG AND C. W. OOSTERLEE, *Multigrid*, Academic Press, London, 2000.

[23]P. WESSELING, *An introduction to multigrid methods*, Pure and Applied Mathematics, John Wiley & Sons, Chichester, 1992.

[24]I. YAVNEH, C. VENNER, AND A. BRANDT, *Fast multigrid solution of the advection problem with closed characteristics*, SIAM J. Sci. Comp., 19 (1998), pp. 111–125.